How the Transition Frequencies of Microtubule Dynamic Instability (Nucleation, Catastrophe, and Rescue) Regulate Microtubule Dynamics in Interphase and Mitosis: Analysis Using a Monte Carlo Computer Simulation

N.R. Gliksman,* R.V. Skibbens, and E.D. Salmon

Department of Biology, University of North Carolina, Chapel Hill, North Carolina 27599-3280

Microtubules (MTs) in newt mitotic spindles grow faster than MTs in the interphase cytoplasmic microtubule complex (CMTC), yet spindle MTs do not have the long lengths or lifetimes of the CMTC microtubules. Because MTs undergo dynamic instability, it is likely that changes in the durations of growth or shortening are responsible for this anomaly. We have used a Monte Carlo computer simulation to examine how changes in the number of MTs and changes in the catastrophe and rescue frequencies of dynamic instability may be responsible for the cell cycle dependent changes in MT characteristics. We used the computer simulations to model interphase-like or mitotic-like MT populations on the basis of the dynamic instability parameters available from newt lung epithelial cells in vivo. We started with parameters that produced MT populations similar to the interphase newt lung cell CMTC. In the simulation, increasing the number of MTs and either increasing the frequency of catastrophe or decreasing the frequency of rescue reproduced the changes in MT dynamics measured in vivo between interphase and mitosis.

INTRODUCTION

There are major differences between microtubule (MT)[1] lengths (Figure 1) and assembly dynamics (Table 1) between the interphase cytoplasmic MT complex (CMTC) and the mitotic spindle. There are fewer MTs in the CMTC (Snyder and McIntosh, 1975; Kuriyama and Borisy, 1981). MTs exhibit slower growth velocities in the CMTC yet achieve much longer average lengths than in mitosis (Rieder, 1977; Kitanishi-Yumura and Fukui, 1987; Cassimeris et al., 1988; Hayden et al., 1990; Aist and Bayles, 1991). The distribution of MT lengths is gausian-like or bell shaped within the CMTC but is a decreasing exponential in the mitotic spindle (Cassimeris et al., 1986; Kitanishi-Yumura and Fukui, 1987; Aist and Bayles, 1991). Turnover rates of tubulin in the

CMTC depend on the distance from the nucleation site (Sammak et al., 1987) but are independent of distance in spindles (Stemple et al., 1988). Finally, MT turnover in the CMTC is two to three orders of magnitude slower than for the dynamic MTs of the mitotic spindle (Wadsworth and Salmon, 1986a; Cassimeris et al., 1988; Joshi et al., 1992).

Changes in MT dynamic instability are thought to be responsible for differences in MT assembly in the interphase CMTC and the mitotic spindle. In both the CMTC and mitotic spindle, MTs are polarized polymers oriented with their "plus" (fast-growing) ends distal from nucleation sites at the centrosomes or spindle poles. MT growth and shortening predominantly occurs at the distal plus ends, although there is some evidence for a steady slow disassembly at the minus ends proximal to the centrosomes (Mitchison, 1989; Sawin and Mitchison, 1991; Mitchison and Salmon, 1992). The great majority of plus ends in the CMTC and the mitotic spindle exhibit dynamic instability, abruptly and stochastically, switching between distinctly different persistent constant velocity phases of elongation (growth)

---

* Present address: Department of Cell Biology, Duke University Medical Center, Durham, NC 27710.
[1] Abbreviations used: CMTC, cytoplasmic microtubule complex; FRAP, fluorescence recovery after photobleaching; M-phase, mitosis or meiosis; MT, microtubule; NLC, newt lung epithelial cell.
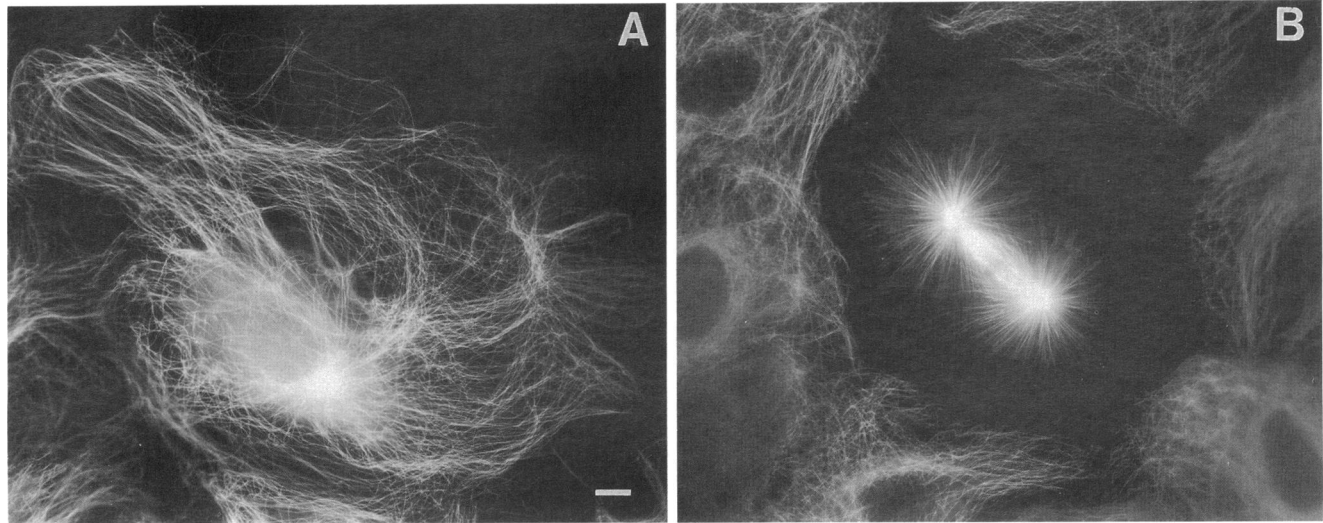
Figure 1. Immunofluorescent micrographs of a newt lung cell interphase CMTC (A) and a mitotic spindle (B). The CMTC has a few hundred MTs of extremely long lengths (A), whereas the spindle contains about 2000 MTs of much shorter length (B). Bar, 10 μm.

and shortening (shrinking) (Salmon, 1989). Kinetochore MTs, which are a minor fraction of spindle MTs, are differentially stable, but their plus ends at the kinetochores also exhibit dynamic instability (Skibbens *et al.*, 1993).

Dynamic instability is an assembly property of free MT ends exhibited both in vivo and in vitro (Mitchison and Kirschner, 1984; Horio and Hotani, 1986; Cassimeris *et al.*, 1988; Sammak and Borisy, 1988; Schulze and Kirschner, 1988; Walker *et al.*, 1988). Five parameters describe the dynamic instability of a microtubule end: elongation velocity, shortening velocity, nucleation frequency, catastrophe frequency, and rescue frequency. When an end is in the elongation state, tubulin association dominates. While in the shortening state, tubulin dissociation dominates. Nucleation is the transition that initiates elongation. Catastrophe is the transition from elongation to shortening, and rescue is the transition from shortening to elongation. No rescue occurs if an end shortens all the way back to the nucleation site. Measurements of the assembly dynamics of individual ends both in vitro and in vivo have shown that catastrophe and rescue are abrupt, stochastic, and generally asynchronous among a population of MTs (Cassimeris *et al.*, 1988; Walker *et al.*, 1988; Belmont *et al.*, 1990; Gliksman *et al.*, 1992). Elongation occurs by the association of tubulin with bound GTP (tubulin-GTP) onto an end in the elongation state. Catastrophe is thought to occur when a growing MT end looses a stabilizing cap of tubulin-GTP subunits. This allows the core of tubulin-GDP subunits to rapidly dissociate producing shortening. Rescue is thought to occur when the end becomes recapped with tubulin-GTP subunits (Mitchison and Kirschner, 1984; Kirschner and Mit-

chison, 1986; Walker *et al.*, 1988, 1991; Bayley *et al.*, 1990; O'Brien *et al.*, 1990; Caplow, 1992).

The dynamic instability parameters of CMTC MTs could be altered kinetically in at least four ways to produce the shorter more dynamic MTs of the mitotic spindle: the velocity during elongation could decrease, the velocity during shortening could increase, the duration of elongation could decrease because of a higher frequency of catastrophe, or the duration of shortening could increase because of a lower frequency of rescue. Of these four possibilities, there is direct evidence that the first two do not occur in vivo. Interphase and mitotic MT elongation and shortening velocities have been measured in newt lung epithelial cells (NLC) (Table 1). The elongation velocity was found to be faster during mitosis than during interphase, and no change in shortening velocity was seen (Cassimeris *et al.*, 1988; Hayden *et al.*, 1990; Spurck *et al.*, 1990). In contrast, there is evidence that both of the last possibilities, increased catastrophe frequency and decreased rescue frequency, contribute to the conversion of CMTC to mitotic MT assembly (Table 1) (Belmont *et al.*, 1990; Gliksman *et al.*, 1992; Verde *et al.*, 1992). At entry to mitosis, activation of the mitotic-promoting factor (MPF or cdc2-cyclin kinase) promotes a phosphorylation cascade inducing mitotic spindle formation. Studies of MT assembly in cytoplasmic extracts have demonstrated that promotion of phosphorylation either by activating MPF or blocking phosphatase activity with okadaic acid induces conversion from interphase-like to mitotic-like MT assembly without major change in either elongation or shortening velocities; these changes were brought about by increased catastrophe or de-

creased rescue frequencies (Belmont *et al.*, 1990; Gliksman *et al.*, 1992; Verde *et al.*, 1992).

In tissue cells, because of their small volume, changes in nucleation may also play a significant role in remolding the assembly dynamics of MTs between interphase and mitosis. In preparation for mitosis, centrosomes in animal cells are replicated to provide the bipolarity of the mitotic spindle. In addition, the mitotic phosphorylation of centrosomal proteins increases the nucleation potential of each centrosome (Snyder and McIntosh, 1975; Kuriyama and Borisy, 1981; Buendia *et al.*, 1992). As Mitchison and Kirschner (1987) have discussed, increasing nucleation within a finite volume of tubulin subunits will increase the amount of polymerization, decreasing the unpolymerized tubulin concentration and slowing MT elongation velocity. Thus, increasing nucleation could indirectly contribute to the shorter MT lengths achieved but could not by itself account for the observed increase in elongation velocities in mitosis.

Computer simulations, based upon Monte Carlo methods of modeling stochastic processes, provide a powerful way of analyzing complex processes like the assembly dynamics of a population of MTs exhibiting dynamic instability within a cell. The transition frequencies of dynamic instability are stochastic, which limits the feasibility of analytical approaches to predict the assembly properties of MT populations or individual MTs within the population (Hill, 1987; Mitchison and Kirschner, 1987; Verde *et al.*, 1992). We based our computer simulations on the parameters of MT dynamic instability available for interphase and mitotic newt lung cells (Figure 1). This cell type currently has the highest number of measured parameters for MT dynamic instability for both the interphase CMTC and the mitotic spindle (Table 1). The simulations were mainly directed at testing how changes in MT assembly are controlled between interphase and mitosis by changes in nucleation and the frequencies of catastrophe and rescue. Nevertheless, the program could also be easily modified to model how MT dynamics change during other types of cell activities.

MATERIALS AND METHODS

Immunofluorescence

Oregon newts (*Taricha granulosa*) were obtained from Charles Sullivan (Nashville, TN). Newt lung cultures were prepared and processed for indirect immunofluorescence as described by Rieder *et al.* (1986) and Cassimeris *et al.* (1988). Micrographs were obtained using a Nikon Optiphot (Garden City, NY) equipped a 60X, 1.4NA PlanApo objective and epi-illuminated with a 100 W mercury bulb. Images were recorded using TMax 100 film (Kodak, Rochester, NY).

General Features of the Simulation Program

We used a Monte Carlo technique to simulate the dynamic instability of individual MT ends as originally described by Gliksman *et al.* (1987) and Bayley *et al.* (1989). The program simulated a population of ≤4000

MTs within a defined cell volume that grew and shortened only at their plus ends following nucleation. The program was written in Turbo Pascal (Version 5.0 Borland International, Scotts Valley, CA) and runs on PC computers. The program is available upon request.

The program specifically assumed that all MT plus ends had identical parameters of dynamic instability and were in one of the following states: elongation, shortening, or no polymer (an empty nucleation site and no MT) (Figure 2). MTs switched between states via one of the following transitions: nucleation (no polymer to elongation), catastrophe (elongation to shortening), or rescue (shortening to elongation). MTs that shortened to zero length automatically switched to the no polymer state.

Several assembly parameters were entered into the program and held constant for each simulation situation. These parameters included: the cell volume, the cellular tubulin concentration, the rate constants of elongation and shortening, the number of nucleation sites, and the frequencies of nucleation, catastrophe, and rescue. Although most of these parameters could be made dependent on tubulin concentration, for this paper we simplified the simulations by making only elongation velocity concentration dependent (see DISCUSSION).

To save time, most of the simulated MT populations were initiated from the no polymer state. Trial runs of the simulation demonstrated that changes in the MT dynamics parameters produced reversible changes in the steady state MT populations; it did not matter whether the MT population had started in the no polymer state or had previously been assembled.

The program ran in cycles representing 1-s periods of MT assembly. This time interval was slightly shorter than the intervals typically used to measure microtubule dynamics both in vitro and in vivo (Cassimeris *et al.*, 1988; Sammak and Borisy, 1988; Schulze and Kirschner, 1988; Belmont *et al.*, 1990; O'Brien *et al.*, 1990; Gliksman *et al.*, 1992; Verde *et al.*, 1992). At the beginning of each cycle, the program measured the concentration of unpolymerized tubulin from which it calculated the current MT elongation velocity. The program determined whether each MT end would undergo a transition by comparing a computer generated random number (0–1) with the transition frequency appropriate for the MT state (nucleation for no polymer, ca-
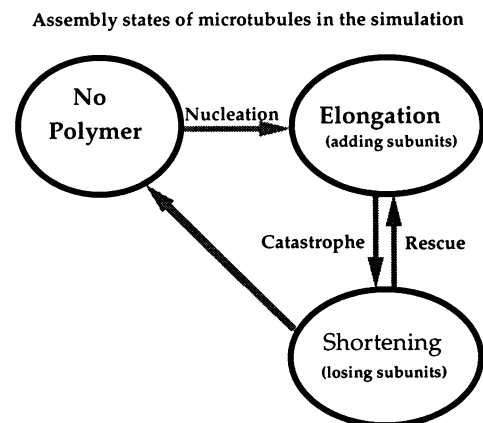
Assembly states of microtubules in the simulation

Figure 2. Plus-end MT assembly states in the Monte Carlo simulation. MTs nucleated from no polymer into the elongation state where the velocity was proportional to the unpolymerized tubulin concentration. MT plus ends stochastically switched (catastrophe) from the elongation state into the shortening state where the velocity was independent of the unpolymerized tubulin concentration. Plus ends in the shortening state either stochastically switched (rescue) back to the elongation state or shortened all the way back to the nucleation site (no polymer state). Each MT plus end was considered independent of the others, but each MT used up tubulin from a common pool of unpolymerized subunits.

tastrophe for elongation, rescue for shortening); a transition occurred if the random number was less than the transition frequency. Transitions were assumed to be instantaneous. Subunits were added to or subtracted from a MT end in proportion to the velocity appropriate for the MT state and the 1-s cycle interval. Simulations were run until populations had achieved steady-state levels of polymer and steady-state average MT lengths.

When assembly reached steady state, the simulation was continued, and the computer monitored the mean MT length, the MT elongation velocity, the distribution of MT lengths, the amount of polymerized and unpolymerized tubulin, the growth dynamics of individual ends, the turnover rates of tubulin at positions along the lengths of MTs, and the turnover rates of whole MTs.

The rates of steady-state tubulin turnover at various positions from the nucleation sites were measured by marking microtubules at these sites. The computer then monitored return of unmarked subunits to the sites. This method is analogous to the fluorescence redistribution after photobleaching or photoactivation experiments performed previously in living cells (Saxton *et al.*, 1984; Salmon *et al.*, 1984; Wadsworth and Salmon, 1986b; Stemple *et al.*, 1988; Mitchison, 1989; Sawin and Mitchison, 1991; Mitchison and Salmon, 1992). The percentage of tubulin turnover within the microtubules at each position was calculated from the ratio of unmarked MTs at that position divided by the number of MTs initially marked at that position. A MT was counted as an unmarked MT only after it both shortened through the mark site loosing its labeled subunits then later elongated back through the mark site with unlabeled subunits.

The rate of whole MT turnover under steady-state assembly conditions was calculated in the following way. After the MT population reached steady state, the nucleation frequency was set to 0 s^{-1}, and the elongation velocity was made constant at the steady-state value, independent of the unpolymerized tubulin concentration. The simulation was then continued, and the number of MT nucleation sites in the no polymer state and the total amount of polymer was monitored. This method allowed us to simultaneously measure steady-state turnover of polymer as well as the turnover of whole MTs. The half-time of MT turnover corresponded to the amount of time (number of cycles) required for at least half of the MTs to reach the no polymer state.

Simulation of Newt Cell MT Assembly

A major goal of our simulations was to model MT assembly dynamics in the cell where the total amount of tubulin is limited by the cell volume and cellular tubulin concentration. The newt cells have a cytoplasmic volume of about 8 pL, on the basis of their diameter when they round-up with trypsin treatment (Rieder, personal communication). There has been no direct measurement of the cellular tubulin concentration in newt cells, but other cell types have been shown to have concentrations of 20–30 μM (Pfeffer *et al.*, 1976; Hiller and Weber, 1978). For our simulations, we obtained an estimate of the newt cellular tubulin concentration in the following way. The interphase CMTC (Figure 1A and Table 1) contains about 500 MTs with an average length of ~100 μm (Rieder and Cassimeris, personal communications). The polymerized tubulin in 500 MTs of 100 μm average length is equivalent to 17 μM concentration in a volume of 8 pL. We assumed, on the basis of measurements in other types of dividing cells (Pipeleers *et al.*, 1977a,b; Hiller and Weber, 1978; Olmsted, 1981), that the amount of polymerized tubulin in interphase was two-thirds of the total amount of tubulin in the cell. This assumption yielded a value of 25.4 μM for the newt cellular tubulin concentration. This value was kept constant during our simulations. The concentration of unpolymerized tubulin was calculated by subtracting the concentration of polymerized tubulin from 25.4 μM.

We set the tubulin association rate constant during the elongation state (Walker *et al.*, 1988) to a value that gave the measured interphase growth rate of 7.2 μm/min (Table 1) at an unpolymerized tubulin concentration of 8.4 μM. This concentration is the difference between a cellular tubulin concentration of 25.4 μM and a polymerized steady

state tubulin concentration of 17 μM. For simplicity, we assumed that tubulin dissociation in the elongation state (Walker *et al.*, 1988) was zero (Mitchison and Kirschner, 1984; Dreschel *et al.*, 1992; Hyman *et al.*, 1992; Simon *et al.*, 1992).

In all of our simulations, the shortening rate was set constant to 17 μm/min, the measured value in newts during both interphase and mitosis (Table 1). Tubulin dissociation in the shortening state is known to be independent of tubulin concentration (Walker *et al.*, 1988, 1991).

The other parameter that was normally constant in our simulations was the probability or frequency of nucleation. Unless otherwise stated, this parameter was set to 1 so that instantaneous nucleation occurred in the next 1-s cycle when a MT was in the no polymer state. We assumed that nucleation was instantaneous because of the nearly instantaneous MT nucleation observed in cytoplasmic extracts (Gliksman *et al.*, 1992).

RESULTS

Simulation of CMTC MT Assembly

To achieve steady-state assembly, we had to modify slightly one of the dynamic instability parameters measured for the newt interphase CMTC (Table 1). The measured values predicted that an average distance of elongation before catastrophe of 8.5 μm (7.2 μm/min $\times$ 1.18 min duration) and an average distance of shortening before rescue of 6.3 μm (17 μm/min $\times$ 0.37 min). At steady-state assembly, the difference between these two values should be zero, but instead the difference predicted net growth (0.9 μm/min). We achieved zero net elongation by slightly increasing the catastrophe frequency from the measured value of .014 s^{-1} (Table 1) to 0.019 s^{-1}. We assumed that the velocities of elongation and shortening were the more accurate measurements. Though we chose to adjust the catastrophe frequency, we could have also achieved zero net elongation by reducing slightly the rescue frequency from the measured value of 0.044 s^{-1} (Table 1) to 0.033 s^{-1}.

The simulation program produced MT populations with steady-state assembly dynamics typical of the interphase CMTC (Figures 3 and 4 and Table 2) using 0.019 s^{-1} for the catastrophe frequency plus the other measured or estimated parameters in Table 1 for the number of MT nucleation sites, the shortening rate and the rescue frequency (Table 2). The mean length of the nucleated MT population was 100 μm, and the MT length distributions were gausian or bell shaped as exhibited by the CMTC in vivo (Cassimeris *et al.*, 1986; Kitanishi-Yumura and Fukui, 1987; Aist and Bayles, 1991). At steady state, two-thirds of the cellular tubulin concentration was polymerized into MTs (17 μM) and growth velocity was equal to the measured value of 7.2 μm/min (Figure 3, Table 2).

Individual MT ends frequently switched to shortening but achieved long lengths because of frequent rescue (Figure 4B). As reported by Sammak *et al.* (1987), in vivo, tubulin turnover within CMTC MTs was dependent on the distance from the nucleating site. Turnover was much slower at positions closer to the nucleation sites (Figure 4C). The average half-time for whole MT

Table 1. MT assembly parameters measured or estimated for the interphase CMTC and the mitotic spindle in newt lung tissue cells

Cell volume	8 pl[a]	
Tubulin	20–30 μM[b]	
	Interphase	Mitosis
Number of microtubules in the cell	200–500[c]	~2 000[c]
Average microtubule length	100 μm[c]	12–14 μm[c,e]
Microtubule dynamic instability		
Elongation rate	7.2 μm/min[d]	14.4 μm/min[e]
Shortening rate	17 μm/min[d]	17 μm/min[e,f]
Time in elongation	71 s[d]	Unknown
Catastrophy frequency	0.014 s^{-1} [d]	Unknown
Time in shortening	22 s[d]	Unknown
Rescue frequency	0.044 s^{-1} [d]	Unknown
Tubulin turnover versus distance	Highly dependent[g]	Unknown
Halftime of tubulin turnover	Unknown	75 s[h]
Average microtubule lifetime	Many minutes[d]	<2 min[e,h]
Predicted length distribution	Bell shaped[i]	Exponentially[j] decreasing

[a] Estimate from trypsinized cells (Rieder, personal communication).

[b] Pfeffer *et al.*, 1976; Hiller and Weber, 1978.

[c] Rieder, 1977; Rieder and Cassimeris, personal communications.

[d] Cassimeris *et al.*, 1988.

[e] Hayden *et al.*, 1990.

[f] Spurck *et al.*, 1990.

[g] Sammak *et al.*, 1987.

[h] Wadsworth and Salmon, 1986a.

[i] Cassimeris *et al.*, 1986; Kitanishi-Yumura and Fukui, 1987; Verde *et al.*, 1990; Aist and Bayles, 1991; Gliksman *et al.*, 1992.

[j] Kitanishi-Yumura and Fukui, 1987; Verde *et al.*, 1990; Aist and Bayles, 1991.

turnover was also very slow (3.5 h) with an average MT lifetime of >6 h (Figures 3 and 4D) as expected for MTs in the CMTC (Joshi *et al.*, 1992).

We conclude that with slight adjustment of the value for catastrophe frequency, the other measured parameters for dynamic instability in vivo predict remarkably well in our simulation the bulk assembly properties of the CMTC (Figure 3 and Tables 1 and 2). We used this interphase model as the starting point to examine how changes in the number of nucleation sites, and the frequencies of catastrophe and rescue alter MT assembly when the remaining parameters of assembly were held constant at their interphase values.

Increasing the Number of Nucleation Sites

We increased the number of MT sites in our interphase model from 500 to 1000, 2000 or 4000 sites to see how increased nucleation altered MT assembly dynamics (Figures 3 and 5). Higher numbers of nucleation sites significantly decreased the mean MT lengths and slightly decreased elongation velocities as net tubulin polymerization increased. Higher numbers of nucleation sites also decreased the half-time of whole MT turnover.

The number of MT nucleation sites in newt cells increases from ~500 in the interphase CMTC to ~2000

in the mitotic bipolar spindle (Table 1). Figure 5 shows that for the 2000 nucleation sites expected in mitosis, the MT length distribution converted from the interphase bell-shape distribution of long MTs, to an exponentially decreasing distribution of short MTs more typical of mitotic cells. Tubulin turnover in the shorter MTs did not depend significantly on distance from the nucleation center as occurred in the long interphase MTs, although the catastrophe and rescue frequencies were still the at interphase values (Figure 5C).

Nevertheless, increasing only the number of nucleation sites did not achieve all aspects expected for mitotic MT assembly. The half-time of whole MT turnover (12 min) was ten times longer than expected for mitotic MTs (1.3 min) (Table 1 and Figure 3). Also, the mean MT length (27 μm) was larger than expected for mitotic MTs (14 μm), and the growth velocity (6 μm/min), in particular, was much slower than the 14 μm/min velocities measured for spindle MTs (Table 1 and Figures 3 and 5).

Increasing the Catastrophe Frequency

If we ran the interphase model but increased catastrophe frequency about threefold from the interphase value of 0.019 to 0.056 s^{-1}, there was a dramatic change in MT
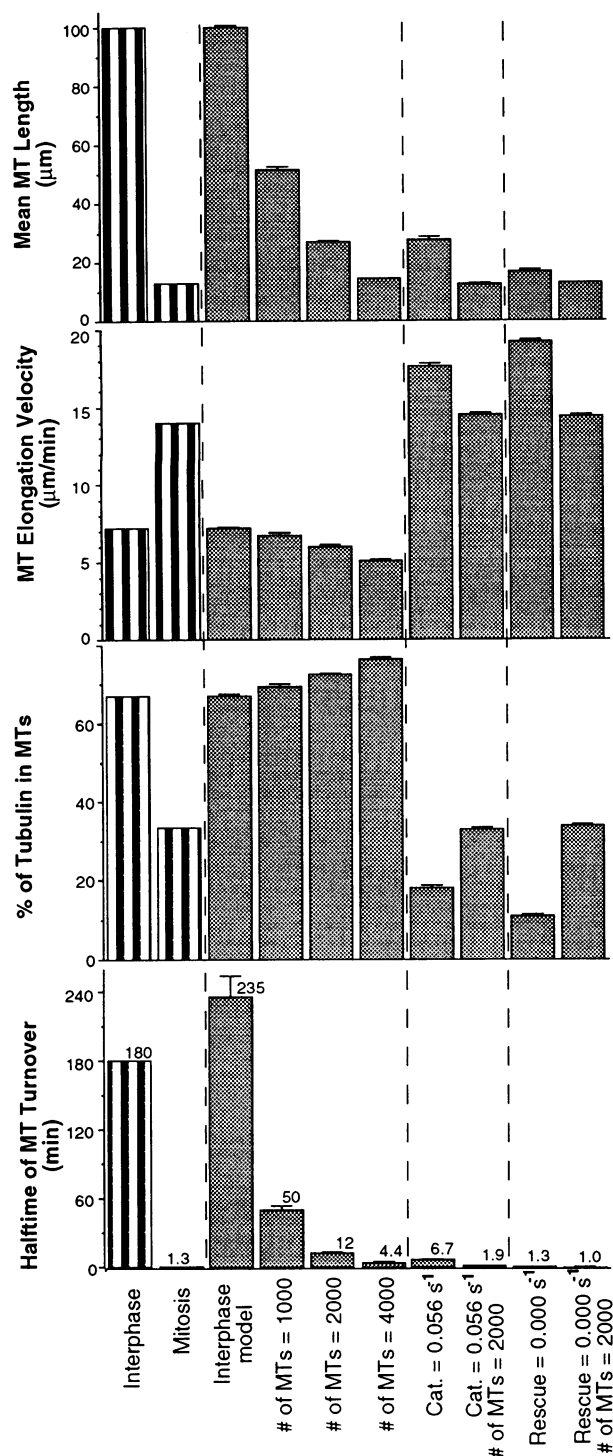
assembly. The mean MT length decreased from 100 to ~25 μm. The elongation velocity increased from 7.2 to 17 μm/min as the percentage of polymerized tubulin decreased. The half-time of MT turnover substantially shortened from 180 to 6.7 min (Figure 3). These results show that increasing catastrophe frequency produces the major features of mitotic MT dynamics: shorter mean length, faster growth rate, and much quicker MT turnover (in comparison to interphase) (Table 1). However, the half-life of MT turnover in mitosis is close to 1 min, not 6.7 min. Higher frequencies of catastrophe shortened the half-life of MT turnover below 6.7 min, but this produced little MT polymer and MT elongation rates much faster than the 14 μm/min typical of mitosis (Figure 3).

If we combined a threefold increase in catastrophe frequency with the 2000 nucleation sites typical of mitosis, then the model came much closer to predicting the newt mitotic MT dynamics (Figures 3 and 6 and Tables 1 and 2). The mean MT length was 12.5 μm. The elongation velocity was about 14.5 μm/min. The half-life of MT turnover was 1.9 min and tubulin turnover within MTs was independent of the distance from the nucleation sites. MT turnover was still not quite as fast or as complete as expected for spindle MTs (1.1 min); however, changing only the two variables in the simulation (increasing the catastrophe frequency threefold and the number of nucleation sites fourfold) produced changes in all other aspects of MT assembly typical of the transition between interphase and mitosis.

Decreasing the Rescue Frequency to Zero

If we ran the interphase model, but made the rescue frequency 0.0 s⁻¹ without changing any of the other interphase parameters, there was also a dramatic change in MT assembly similar to the response produced by increasing catastrophe frequency, as described above. The mean MT length decreased from 100 to ~18 μm. The elongation velocity increased from 7.2 μm/min to 19 μm/min as the concentration of tubulin in MTs decreased. The half-time of MT

Figure 3. Comparison of the assembly characteristics of MT arrays in vivo with MT arrays in the computer simulations. Striped columns are values thought to represent interphase or mitotic cells in vivo (Table 1). The eight gray columns represent the eight different sets of nucleation and dynamic instability parameters used for simulations. The interphase model corresponds to the interphase parameters in Table 2; 500 MTs were assembled with a catastrophe frequency of 0.019 s⁻¹ and a rescue frequency of 0.044 s⁻¹. The next three columns correspond to models in which the catastrophe and rescue frequencies

were held at their interphase values while the number of MT sites was increased to 1000, 2000, and 4000 MTs, respectively. The next two columns correspond to models in which the rescue frequency was held at its interphase value while the catastrophe frequency was increased from 0.019 to 0.056 s⁻¹ with either 500 or 2000 MT sites, respectively. The last two columns correspond to models in which the catastrophe frequency was held at its interphase value while the rescue frequency was decreased from 0.044 to 0.000 s⁻¹ with either 500 or 2000 sites used, respectively. Each gray bar is the mean of at least four simulated MT populations, and error bars represent SD. Individual half-times of whole MT turnover are listed for each model. The cell volume, the MT shortening velocity, the total concentration of tubulin, and the tubulin association rate and tubulin dissociation rate during elongation were all held constant at the values listed in Table 2.
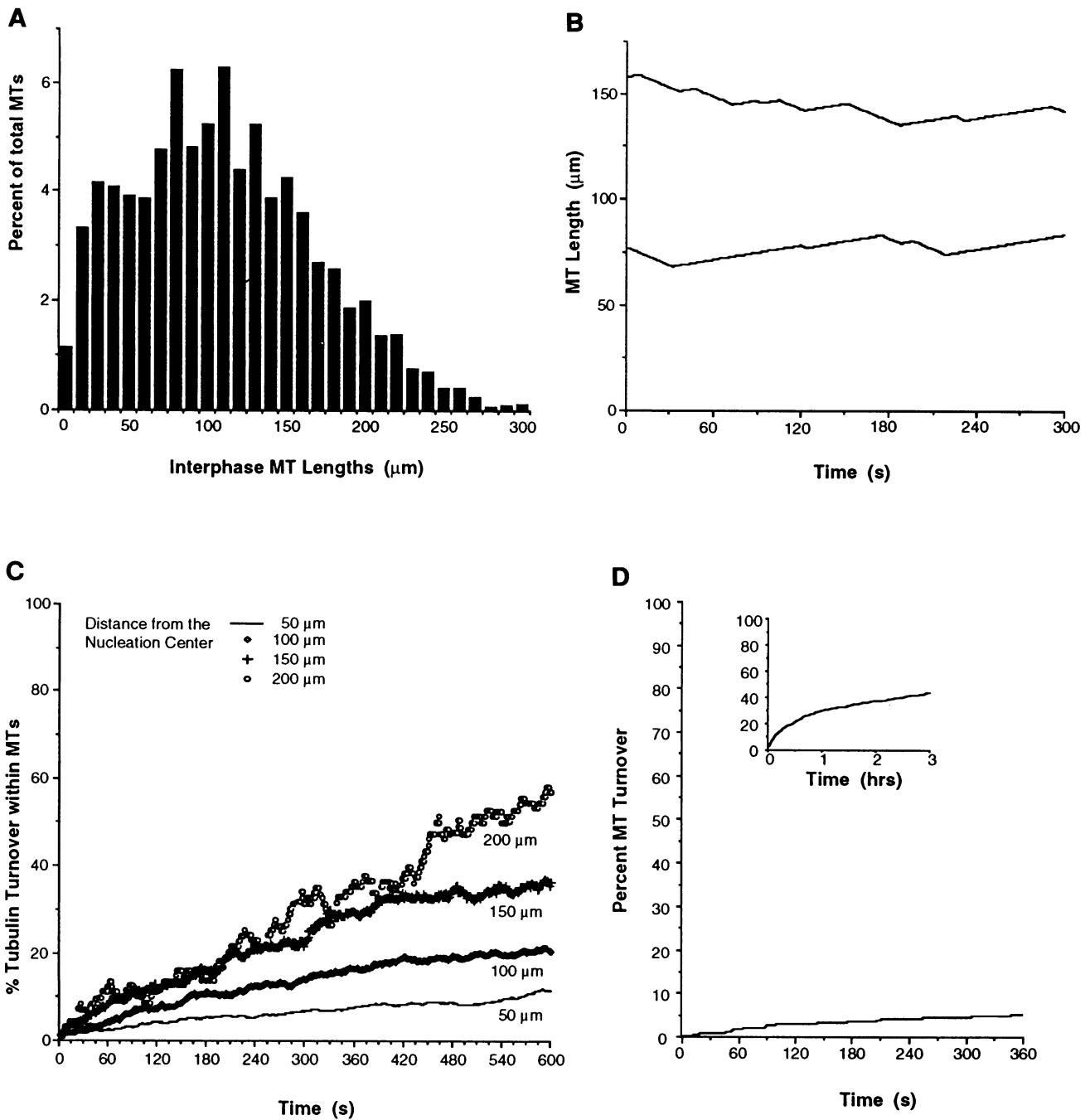
Simulation of interphase MT assembly

Figure 4. Simulation of interphase CMTC assembly. Populations of 500 MTs were assembled to reach a steady-state mean length and steady-state polymer concentration using the interphase model parameters shown in Table 2. The MT length histogram is an average of three simulated populations (A). B shows the length histories of simulated MTs. Tubulin turnover was measured by simulating lattice marking experiments at 0.5, 1, 1.5, and 2 times the mean MT length away from the nucleation site (C). Whole MT turnover was measured under steady-state conditions (D).

turnover substantially shortened from 180 min to 1 min (Figure 3). These results show that making rescue zero, like increasing the catastrophe frequency three-fold, produces the major features of mitotic MT dy-

namics (Table 1). The half-life of MT turnover was nearly identical to the value measured in the mitotic spindle (Figure 3 and Table 1); however, the elongation velocities were higher and the percentage of

Table 2. Microtubule populations produced by the Monte Carlo computer simulation by varying the dynamic instability parameters[a]

	Interphase model	Increased number of microtubules (2 000)	Increased catastrophe frequency and 2 000 microtubules	Increased rescue frequency and 2 000 microtubules
Model results shown in:	Figure 4	Figure 5	Figure 6	Figure 7
Dynamic instability parameters:				
Number of microtubules	500	2 000	2 000	2 000
Catastrophy frequency (s^{-1})	0.019	0.019	0.056	0.019
Rescue frequency (s^{-1})	0.044	0.044	0.044	0.000
Mean average microtubule length (μm) [n]	100.0 ± 0.6 [16]	27.1 ± 0.1 [14]	12.5 ± 0.2 [10]	12.7 ± 0.1 [13]
Mean elongation rate (μm/min) [n]	7.2 ± 0.1 [16]	6.0 ± 0.1 [14]	14.5 ± 0.1 [10]	14.4 ± 0.1 [13]
Mean steady-state polymer concentration (μM) [n]	17.0 ± 0.1 [16]	18.4 ± 0.1 [14]	8.4 ± 0.2 [10]	8.6 ± 0.1 [13]
Tubulin turnover versus distance from the pole	Highly dependent	Independent	Independent	Independent
Half-time of tubulin turnover at the average length [n]	>3 h [4]	>6 min [4]	108 ± 11 s [10]	57 ± 4 s [7]
Half-time of whole microtubule turnover [n]	14 114 ± 1 144 s > 3.5 h [4]	738 ± 39 s >10 min [4]	121 ± 2 s ~2 min [4]	65 ± 2 s ~1 min [4]
Estimated average microtubule lifetimes	5.6 h	17.7 min	3 min	1.5 min
Shape of length distribution	Bell shaped	Decreasing	Decreasing	Decreasing

[a] Constants: All simulation populations were initiated with microtubules having 0 length and in the no polymer state. The total tubulin concentration was 25.44 μM. The total volume was 8 pl. The association rate of tubulin during microtubule elongation (K_{e2}) was 0.85 μm/ min/μm. The dissociation rate of tubulin during microtubule elongation (K_{e-1}) was 0 μm/min. The rate of microtubule shortening rate was 17 μm/min.

polymerized tubulin was much lower than expected for mitosis (Figure 3).

If we combined a rescue frequency of zero with nucleation of 2000, then this model also came much closer to predicting newt mitotic MT dynamics (Figures 3 and 7 and Tables 1 and 2). The mean MT length was 12.7 μm. The elongation velocity was ~14.4 μm/min. The half-life of MT turnover was 0.95 min, and tubulin turnover within MTs was independent of the distance from the nucleation sites. MT turnover was slightly faster than measured for spindle MTs, but in all other aspects changing only two variables in the simulation (making the rescue frequency zero and increasing the number of nucleation sites fourfold) produced changes in MT assembly typical of the transition between interphase and mitosis.

Changes in Catastrophe Versus Rescue Needed to Achieve Mitotic Assembly

We also examined the cooperative effects of changing both catastrophe and rescue frequencies, because it is possible that catastrophe increases and rescue decreases upon entry into mitosis (Cassimeris *et al.*, 1988; Belmont *et al.*, 1990; Gliksman *et al.*, 1992; Verde *et al.*, 1992). We increased the number of MT nucleation sites to 2000 in the interphase model, then determined the combination of values for the frequencies of catastrophe and rescue that produced a steady-state average MT length between 12 and 13 μm, the value typical of NLC mitotic MTs. The results from these simulations showed that

there was a linear relationship between the changes in catastrophe and rescue frequencies required to achieve the short MTs of the mitotic spindle as shown in Figure 8.

Kinetics of Conversion Between Interphase and Mitotic Assembly

The last of our experiments examined the time course of the conversion from the interphase CMTC into the mitotic spindle and the reverse, the conversion from the mitotic spindle into the interphase CMTC. MTs were assembled to steady state using the interphase model (Figure 4). Abruptly, the number of MT nucleation sites was increased (from 500 to 2000) and the catastrophe frequency was increased about threefold (from 0.019 to 0.056 s^{-1}) or the rescue frequency was decreased to zero. In either case, the average length of the original 500 MTs decreased progressively until a steady state was reached (Figure 9A). The decrease in average length occurred with a half-time of ~10 min when catastrophe was increased and ~4 min when rescue was reduced to zero. At the new steady-state assembly the average length of the original 500 MTs was equal to the average length of the entire mitotic MT population.

When the simulation parameters were abruptly returned to the original interphase values, the average length of the original 500 MTs increased exponentially back to 100 μm (Figure 9B). The half-life of length recovery was ~7 min for either of the mitotic models.

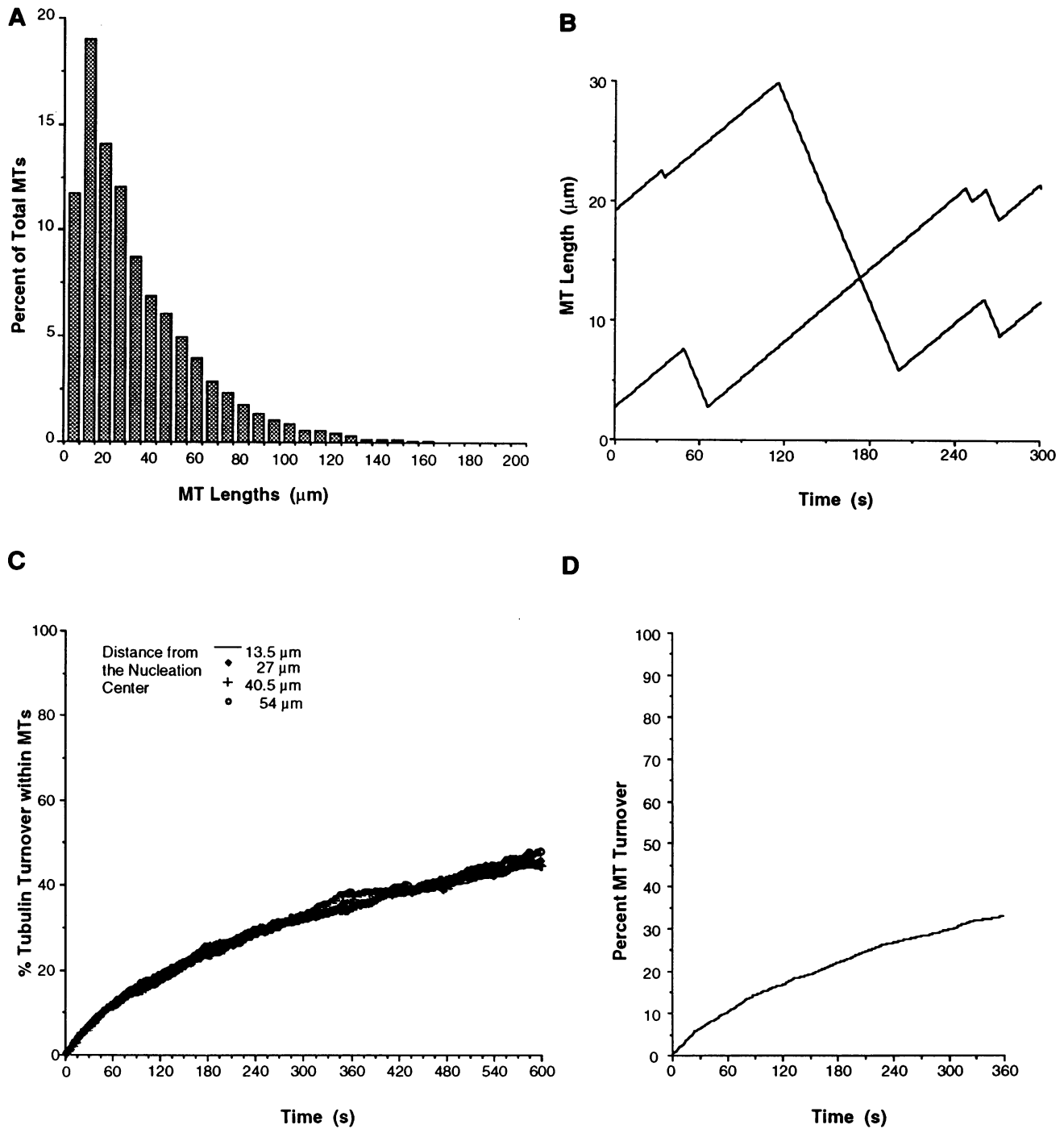# Changes produced by increasing the number of MTs

Figure 5. Changes produced by increasing nucleation to 2000. Starting with the interphase-like model (Figure 4), the number of MT sites was increased from 500 to 2000 MTs without changing the rest of the parameters (see Table 2). Data in A–D were obtained as described in Figure 4.

Changes produced by increasing the catastrophe frequency and the number of MTs
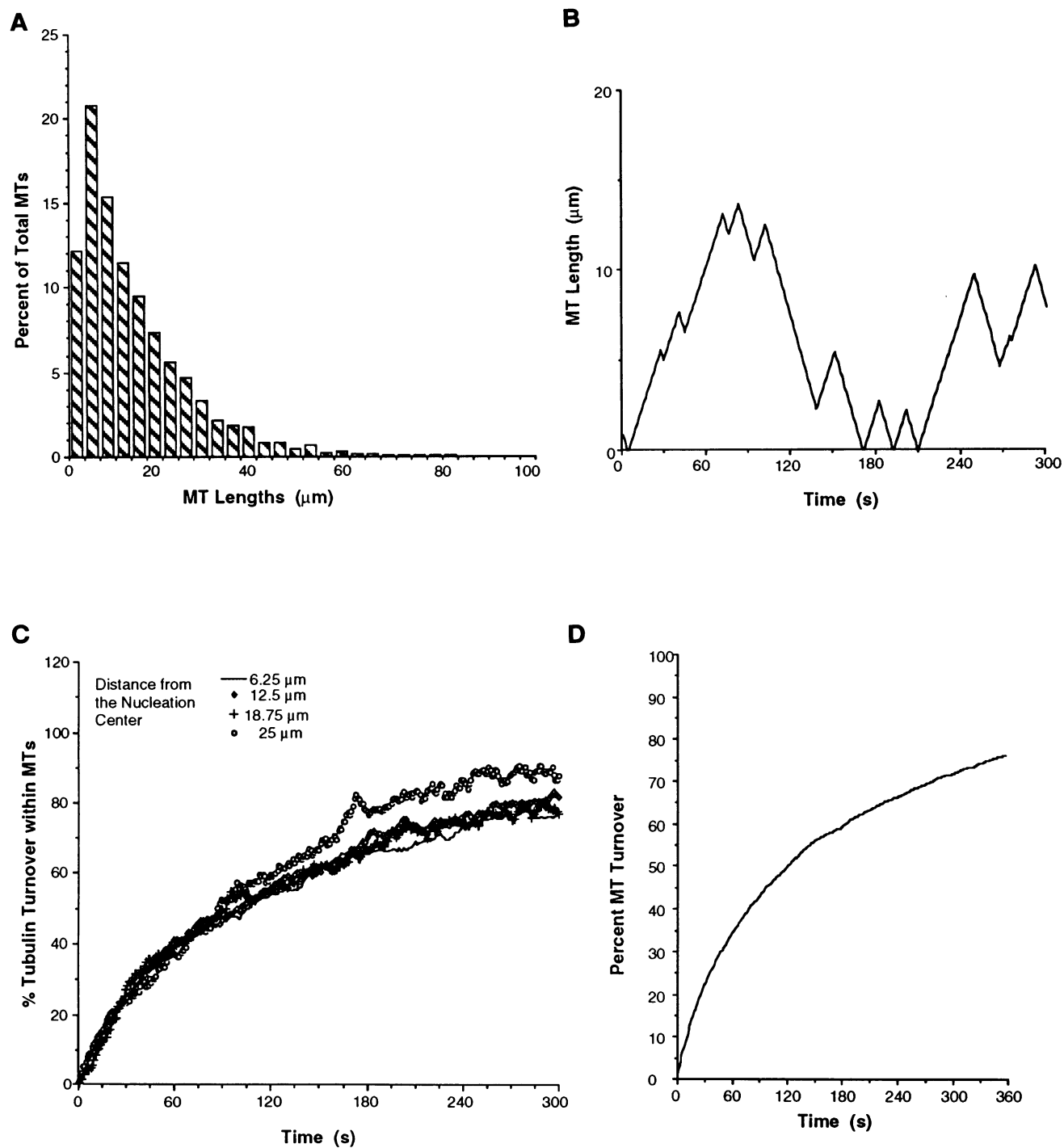
A

B

C

D

Figure 6. Changes produced by increasing catastrophe frequency threefold and nucleation to 2000. Starting with the interphase-like model (Figure 4), the catastrophe frequency was increased from 0.019 to 0.056 s^{-1}, and the number of MT sites was increased from 500 to 2000 MTs without changing the rest of the parameters (see Table 2). Data in A–D were obtained as described in Figure 4.

Changes produced by decreasing the rescue frequency and increasing the number of MTs
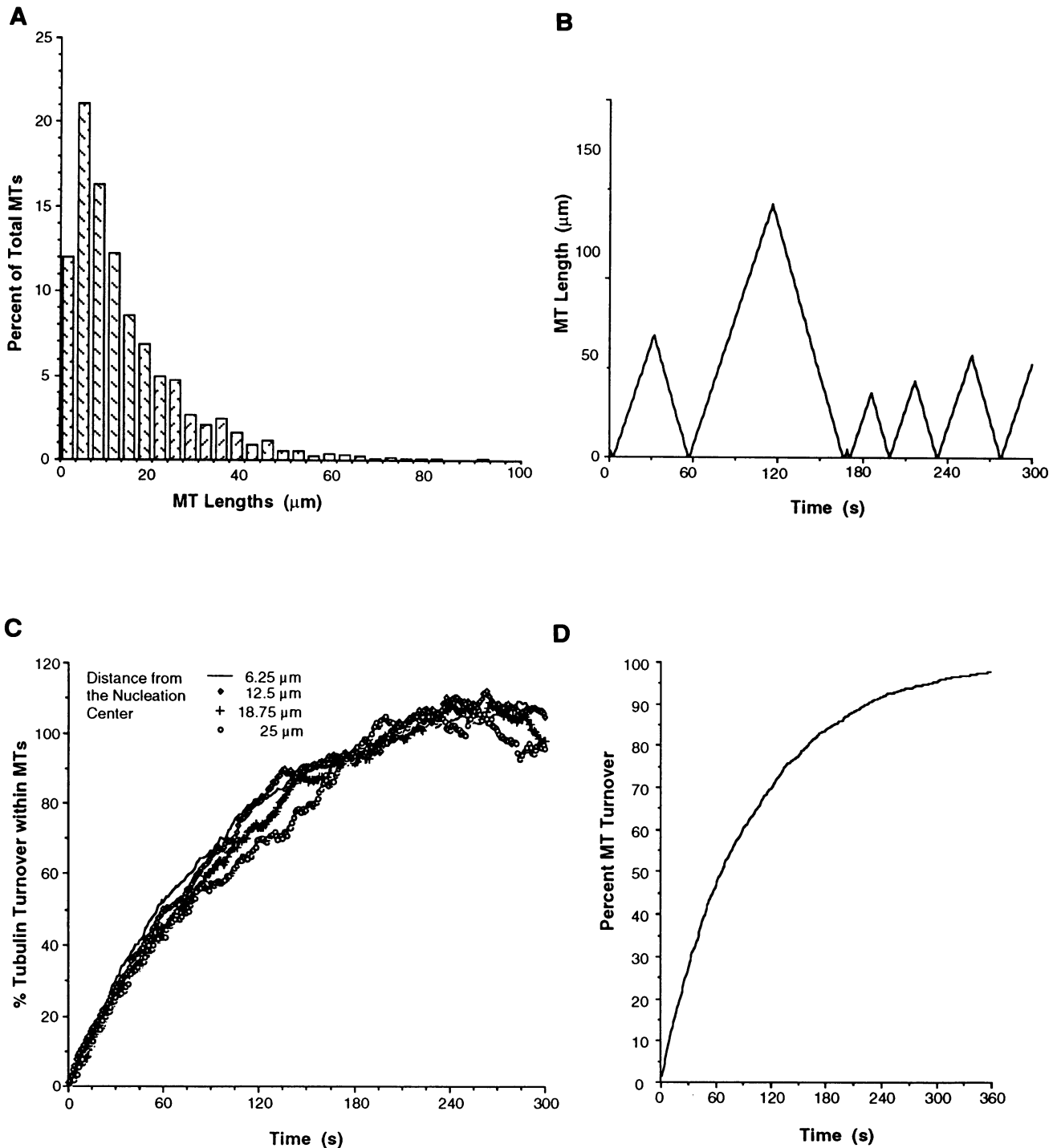

Figure 7. Changes produced by making rescue frequency zero and nucleation 2000. Starting with the interphase-like model (Figure 4), the rescue frequency was decreased from 0.044 to 0.000 s^{-1}, and the number of MT sites was increased from 500 to 2000 MTs without changing the rest of the parameters (see Table 2). Data in A–D were obtained as described in Figure 4.
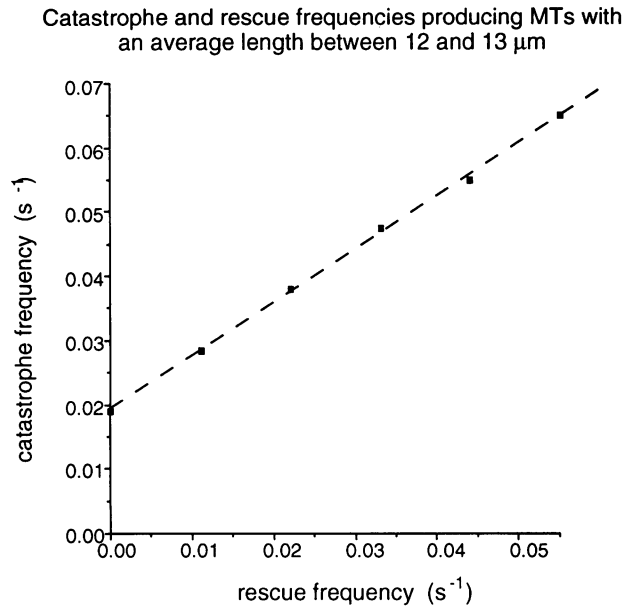

Catastrophe and rescue frequencies producing MTs with an average length between 12 and 13 μm

Figure 8. Catastrophe and rescue frequencies producing MT populations with an average length between 12 and 13 μm. Starting with the interphase-like model (Figure 4), nucleation was increased from 500 to 2000, and rescue frequency was set to various values. The catastrophe frequency was varied without changing the rest of the interphase parameters until an average length between 12 and 13 μm was achieved at steady-state assembly. The straight line through the data was obtained by linear regression.

DISCUSSION

Assumptions Made in Using the Computer Programs

The simulation model described in this paper assumed that MT polymerization reactions occur only at plus ends and that plus ends could only be in the states of no polymer, elongation, or shortening. This precluded other assembly states such as a pause, a state of neither lengthening nor shortening. MT pausing has been noted both in vitro (Walker *et al.*, 1988; Simon *et al.*, 1992) and in vivo (Sammak and Borisy, 1988; Shelden and Wadsworth, 1993) but was rare in interphase newt cells (Cassimeris *et al.*, 1988) and in interphase sea urchin egg cytoplasmic extracts (Gliksman *et al.*, 1992). Our simulation also neglected MT annealing (Rothwell *et al.*, 1986), MT severing (Vale, 1991), nonnucleated MT self-assembly, and any minus-end polymerization or depolymerization (Mitchison, 1989; Sawin and Mitchison, 1991; Mitchison and Salmon, 1992) at the nucleation sites. Given our current state of knowledge about MT assembly in the cell, nucleation, and plus-end dynamic instability appear to be the dominate factors in regulating changes in MT assembly in the cell cycle. If future evidence shows that one of these other assembly states is of interest, it should be fairly easy to modify our computer model to include it in the simulation.

To set up the interphase simulation model, we assumed that assembly was steady state and that two-thirds of the cellular tubulin was on average in polymer and one-third in monomer. We chose a value >50% because we also assumed that the doubling of the MT elongation velocity during mitosis was due to a doubling of the concentration of unpolymerized tubulin rather than an increase in the tubulin association rate during elongation. If <50% of the tubulin was polymerized in the CMTC, the increase in the MT elongation velocity during mitosis would have to involve a more complex mechanism. The above reasoning yielded a value for the tubulin association rate constant in the elongation
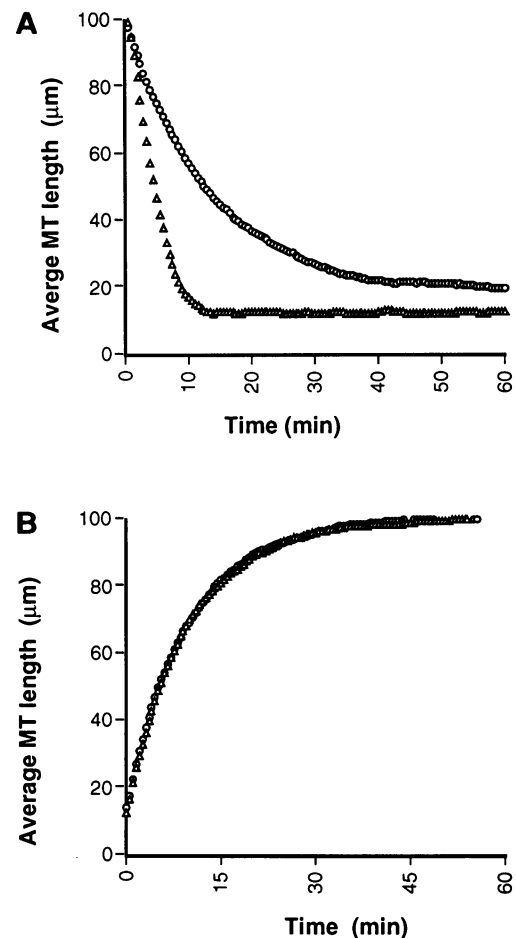

Figure 9. The time course of the conversion from the interphase CMTC into the mitotic spindle and back to the interphase CMTC. (A) MTs were assembled to steady state using the interphase model parameters shown in Table 2. At time 0, the simulation parameters were changed to those of the catastrophe model (O) or the rescue model (△) for mitotic MT assembly (see Table 2). The average MT lengths are those of the original 500 MT nucleation sites and represent the average of three experiments. (B) MTs were assembled to steady state using the catastrophe model (O) or the rescue model (△) for mitotic MT assembly (see Table 2), and at time 0, the simulation parameters were changed to those of the interphase model. The average MT lengths are those of 500 MTs assembled from the catastrophe model (O) or the rescue model (△) and represent the average of three experiments.

state of $2.3 \times 10^7 \, M^{-1}s^{-1}$ to produce $7.2 \, \mu m/min$ growth velocity from $8.1 \, \mu M$ unpolymerized tubulin. This association rate constant is similar to the value estimated for MT growth in sea urchin egg cytoplasmic extracts (Simon et al., 1992).

The frequency of nucleation, catastrophe and rescue were treated as independent variables that were held constant despite changes in the unpolymerized tubulin concentration for either the interphase or mitotic simulations. These transitions frequencies have been shown to depend on the concentration of unpolymerized tubulin for the assembly of pure tubulin in vitro. (Walker et al., 1988, 1991; O'Brien et al., 1990; Voter et al., 1991; Simon et al., 1992). Increasing the concentration of unpolymerized tubulin has been shown to promote nucleation, suppress catastrophe, and may enhance rescue (Walker et al., 1988, 1991; O'Brien et al., 1990; Voter et al., 1991; Simon et al., 1992). The unpolymerized tubulin concentrations in our mitotic simulations were about double that of the interphase simulations accounting for the doubling of the elongation velocity. On the basis of the in vitro studies, this increase in unpolymerized tubulin concentration would be expected to enhance mechanisms that promote nucleation but antagonize the mechanisms that promote catastrophe and decrease rescue.

One other assumption of our simulations was that the dynamic instability parameters and the tubulin concentration did not depend on position within the cell volume nor on distance from the nucleation center. These assumptions seem to be a reasonable first approximation given our current state of knowledge about conditions in the cell. And indeed, the interphase and mitotic simulations predicted the major features expected of in vivo MT assembly.

Changes in Nucleation Effect Steady-State MT Assembly

The number of nucleation sites and the nucleation frequency are typically not included in discussions of the parameters of dynamic instability; nevertheless, nucleation can alter steady state MT assembly. As seen in Figure 3, increasing the number of nucleation sites promotes MT polymerization because there are more MT growing sites. This increase in polymerization depletes the unpolymerized tubulin concentration, slowing the elongation rate. Slowing the elongation rate makes shorter MTs. As the MTs become shorter, they become more dynamic because an increasing number of the MTs shorten all the way back to the nucleation site before a rescue can occur. In this way, increasing the number of nucleation sites yields shorter, more dynamic (shorter half-life) MTs (Figure 3).

Blocking Nucleation Would Have a Slow Effect on CMTC Assembly, but a Very Rapid Effect on Spindle Assembly

The long interphase CMTC MTs in our simulations (Figure 4B) rarely shortened all the way back to the

nucleation site in comparison to the short dynamic mitotic MTs (Figures 6B and 7B). Compare, for example, the very slow rate (3.5-h half-life) of whole MT turnover for the CMTC in Figure 4D to the fast rates (60–70 s) for the mitotic simulations in Figures 6D and 7D. If all MT renucleation was blocked, the half-life of MT loss in the CMTC would be on the order of hours, but the half-life of MT loss during mitosis would be on the order of minutes. Recently, Joshi et al. (1992) have reported that antibodies to gamma-tubulin bind to centrosomes and block MT nucleation. When microinjected into tissue cells, these antibodies were reported to have little noticeable effect on the assembly of the interphase CMTC for ≥ 2 h after injection. In controls, they produced disassembly of the mitotic spindle within 15 min. The difference in the response of the CMTC and spindle is exactly the difference predicted by our simulations.

Why the MT Elongation Velocity Increases Twofold in Mitotic NLCs, but not in Cytoplasmic Extracts

The addition of cyclins to Xenopus interphase egg extracts or okadaic acid to interphase sea urchin egg extracts has been used to create mitotic-like MT populations in vitro (Belmont et al., 1990; Verde et al., 1990, 1992; Gliksman et al., 1992) by increasing the catastrophe frequency or decreasing the rescue frequency. These treatments increased MT elongation velocities by only 10–40% in the extract systems (Belmont et al., 1990; Gliksman et al., 1992; Verde et al., 1992). In contrast, in our cellular simulation, similar increases in catastrophe and or decreases in rescue frequencies doubled the MT elongation velocity. A major difference between the assembly conditions used for the cytoplasmic extract experiments and for our cellular simulations is the concentration of nucleation sites relative to the total tubulin concentration. In the extract experiments, the ratio of nucleation sites relative to the total tubulin concentration was very low in comparison to the ratio in our cellular simulations. In the extracts, the interphase dynamic instability parameters were measured before MT assembly reached a steady-state level. As a result, most of the total tubulin concentration remained unpolymerized, and there was little difference in growth velocity in the extracts for either the interphase or mitotic states. In our cellular simulations, a major fraction of the tubulin pool was polymerized into the CMTC, as occurs in vivo. Under mitotic conditions, the polymerized fraction decreases twofold, doubling the unpolymerized tubulin concentration and elongation velocity.

The Rates of Conversion Between Interphase and Mitotic MT Assembly

The data in Figure 9A show that the rate of conversion from interphase to mitotic assembly is three to four times faster for the rescue model in comparison to the catastrophe model. Conversion is complete within 10 min

for the rescue model, whereas it takes 40 min to achieve mitotic MT lengths with the catastrophe model. Thus, decreasing rescue more rapidly leads to shorter MTs in comparison with increased catastrophe.

In dividing tissue culture cells, most of the interphase MTs have disappeared within 10–15 min after entry into mitosis at nuclear envelope breakdown (Vandre and Borisy, 1985). In rapidly dividing cells like sea urchin embryos, mitosis can be as short as 10 min. This comparison between our simulation results and the in vivo situation indicates that for cell types with short mitotic periods and long CMTC MTs the rescue model, but not the catastrophe model, may be sufficient to explain the interphase to mitosis conversion rate. In other cell types with longer mitotic periods or shorter CMTC MTs, the catastrophe model may be more important because rescues occur infrequently before shortening all the way back to the nucleation site. Faster conversion might also be produced by mitotic activation of MT severing factors recently identified by Vale and coworkers (Vale, 1991).

The data in Figure 9B show that it takes ~20 min to convert to interphase MT assembly from the mitotic state for either the catastrophe or rescue models. This rate of conversion appears similar to the rate in mammalian tissue culture cells, but insufficient in vivo data is available for an accurate comparison.

How Do the Simulation Results Fit Previous Mathematical Models of MT Assembly?

Several mathematical models have been used to predict the bulk assembly properties of populations of MTs undergoing dynamic instability (Hill, 1987; Mitchison and Kirschner, 1987; Bayley *et al.*, 1989; Verde *et al.*, 1992). The results of computer simulations described in this paper fit most of predictions of the previous models and made fewer assumptions about microtubule dynamics.

Mitchison and Kirschner (1987) assumed that MT shortening was instantaneous and that rescue transitions did not occur (i.e., the rescue frequency was 0.0 s^{-1}). Given these assumptions, they found that increased numbers of MT nucleation sites, as occurs during mitosis, should decrease MT lengths, increase the total amount of MT polymer, and decrease MT lifetimes. The results of our simulations shown in Figure 3 fit this prediction despite the presence of rescue and noninstantaneous MT shortening in the model. Nonetheless, MT elongation velocity increases during mitosis, and their model does not predict this result. Either the catastrophe frequency must increase or the rescue frequency must decrease to achieve the fast MT elongation velocity typical of mitosis.

Both Hill (1987) and Verde *et al.* (1992) derived formulas to predict the mean lengths of "bounded" MT populations. By their definitions, a bounded MT population exhibits steady-state assembly when the rate of

polymerization equals the rate of depolymerization for the population; an "unbounded" MT population exhibits net polymerization. In addition, a MT population would be considered bounded if the average length of elongation predicted by elongation velocity and catastrophe frequency was less than the average length of shortening predicted by the shortening velocity and rescue frequency.

For the bounded situation, Hill (1987) and Verde *et al.* (1992) formulated an equation for the average MT length (l_{av}) at steady state assembly:

$$l_{av} = V_e V_s / (V_s k_c - V_e k_r) \qquad (1)$$

where V_e and V_s are the elongation and shortening velocities and k_c and k_r are the catastrophe and rescue frequencies.

Equation 1 was highly inaccurate in predicting average MT length for our interphase model at steady-state assembly, a bounded situation by the bounded definition. In the model, MTs rarely disassembled all the way back to the nucleation site before a rescue occurred. As a result, steady-state assembly was achieved when net elongation equaled net shortening as predicted by the dynamic instability parameters ($V_e/k_c = V_s/k_r$). This equality makes the denominator of Equation 1 go to zero and l_{av} go to infinity. Both in vivo and in our computer simulation l_{av} was about 100 μm at steady-state assembly. In addition, Verde *et al.* (1992) predicted that bounded MT populations would have exponentially decreasing length distributions. In our interphase model and in vivo (Cassimeris *et al.*, 1986; Kitanishi-Yumura and Fukui, 1987; Aist and Bayles, 1991), the steady-state length distribution was bell- or Gaussian-shaped (Figure 4), the distribution they predict for the unbounded state.

In contrast, Equation 1 does predict accurately (within 10%) the average steady state MT lengths and the exponentially decreasing length distributions exhibited by our mitotic simulations (Figures 6 and 7). Unlike the interphase model where the dynamic instability parameters predict net elongation equal to net shortening, the mitotic models predicted that net elongation would be much less than net shortening if MTs were infinitely long and did not disappear by depolymerization to the nucleation site. Thus $V_s k_c - V_e k_r$ from Equation 1 is not near zero as in the interphase model, and Equation 1 provides a reasonable prediction of average mitotic MT length.

Equation 1 can be rewritten to show the relationship between the catastrophe and rescue frequencies for mitotic MT arrays:

$$k_c = (V_e/l_{av}) + k_r(V_e/V_s) \qquad (2)$$

Equation 2 predicts a linear relationship between the values of catastrophe and rescue frequencies for given steady-state values of average length, elongation and

shortening velocities. This linear relationship was demonstrated in Figure 8 for mitotic-like bounded conditions.

The computer simulation model demonstrated that the measured interphase dynamic instability parameters, adjusted slightly to give a steady-state situation, reproduced MT populations with many of the characteristics of the CMTC. In vivo, phosphorylation of the centrosome at mitosis increases the number of MTs in the cell; the simulation model has demonstrated that the increased number of MTs promotes a decrease in MT lengths and an increase in MT turnover but does not account for the increase in MT elongation velocity (Figures 3 and 5). Thus our model predicts that there must be changes in the transition frequencies. Increasing the frequency of catastrophe and decreasing the frequency of rescue both generated similar MT populations with many of the characteristics of the spindle (Figures 3, 6, and 7). Changes in either parameter altered MT lengths, MT elongation velocities, and MT turnover. There were, however, subtle numerical differences between the catastrophe and rescue models. Since direct analysis of single MT dynamics is extremely difficult in the mitotic spindle, future investigations may be able to use the subtle numerical differences between these different models to investigate the CMTC to spindle conversion in other cell types.

ACKNOWLEDGMENTS

REFERENCES

Aist, J.R., and Bayles, C.J. (1991). Ultrastructural basis of mitosis in the fungus Nectria haematococca (sexual stage of Fusarium solani). II Spindles. Protoplasma 161, 123–136.

Bayley, P.M., Schilstra, M.J., and Martin, S.R. (1989). A simple formation of microtubule dynamics: quantitative implications of the dynamic instability of microtubule populations in vivo and in vitro. J. Cell Sci. 93, 241–254.

Bayley, P., Schilstra, M., and Martin, S. (1990). The lateral cap model of microtubule dynamic instability. J. Cell Sci. 95, 33–48.

Belmont, L.D., Hyman, A.A., Sawin, K.E., and Mitchison, T.J. (1990). Real-time visualization of cell cycle-dependent changes in microtubule dynamics in cytoplasmic extracts. Cell 62, 579–589.

Buendia, B., Draetta, G., and Karsenti, E. (1992). Regulation of the microtubule nucleating activity of centrosomes in Xenopus egg extracts: role of cyclin A-associated protein kinase. J. Cell Biol. 116, 1431–1442.

Caplow, M. (1992). Microtubule dynamics. Curr. Opin. Cell Biol. 4, 58–65.

Cassimeris, L.U., Pryer, N.K., and Salmon, E.D. (1988). Real-time observations of microtubule dynamic instability in living cells. J. Cell Biol. 107, 2223–2231.

Cassimeris, L.U., Wadsworth, P., and Salmon, E.D. (1986). Dynamics of microtubule depolymerization in monocytes. J. Cell Biol. 102, 2023–2032.

Dreschel, D.N., Hyman, A.A., Cobb, M.H., and Kirschner, M.W. (1992). Modulation of the dynamic instability of tubulin assembly by the microtubule-associated protein tau. Mol. Biol. Cell 3, 1141–1154.

Gliksman, N.R., Parsons, S.F., and Salmon, E.D. (1992). Okadaic acid induces interphase to mitotic-like microtubule dynamic instability by inactivating rescue. J. Cell Biol. 119, 1271–1276.

Gliksman, N.R., Salmon, E.D., and Walker, R.A. (1987). Relating the kinetic parameters of dynamic instability to the cell: a computer simulation approach. J. Cell Biol. 105, 30a.

Hayden, J.H., Bowser, S.S., and Rieder, C.L. (1990). Kinetochores capture astral microtubules during chromosome attachment to the mitotic spindle: direct visualization in live newt lung cells. J. Cell Biol. 111, 1039–1045.

Hill, T.L. (1987). Linear aggregation theory in cell biology. Springer Series in Molecular Biology, ed. Alexander Rich, New York: Springer-Verlag.

Hiller, G., and Weber, K. (1978). Radioimmunoassay for tubulin: a quantitative comparison of the tubulin content of different established tissue culture cells and tissues. Cell 14, 795–804.

Horio, T., and H. Hotani. (1986). Visualization of the dynamic instability of individual microtubules by darkfield microscopy. Nature 321, 605–607.

Hyman, A.A., Salser, S., Drechsel, D.N., Unwin, N., and Mitchison, T.J. (1992). Role of GTP hydrolysis in microtubule dynamics: information from a slowly hydrolyzable analogue, GMPCPP. Mol. Biol. Cell 3, 1155–1167.

Joshi, H.C., Palacios, J., McNamara, L., and Cleveland, D.W. (1992). γ-tubulin is a centrosomal protein required for cell cycle-dependent microtubule nucleation. Nature 356, 80–83.

Kirschner, M.W., and Mitchison, T.J. (1986). Beyond self assembly: from microtubules to morphogenesis. Cell 45, 329–342.

Kitanishi-Yumura, T., and Fukui, Y. (1987). Reorganization of microtubules during mitosis in Dictyostelium: dissociation from MTOC and selective assembly/disassembly in situ. Cell Motil. 8, 106–117.

Kuriyama, R., and Borisy, G.G. (1981). Microtubule-nucleating activity of centrosomes in CHO cells is independent of the centriole cycle, but coupled to the mitotic cycle. J. Cell Biol. 91, 822–826.

Mitchison, T.J. (1989). Polewards microtubule flux in the mitotic spindle: evidence from photoactivation of fluorescence. J. Cell Biol. 109, 637–652.

Mitchison, T.J., and Kirschner, M. (1984). Dynamic instability of microtubule growth. Nature 312, 237–242.

Mitchison, T.J., and Kirschner, M. (1987). Some thoughts on the partitioning of tubulin between monomer and polymer under conditions of dynamic instability. Cell Biophys. 11, 35–55.

Mitchison, T.J., and Salmon, E.D. (1992). Poleward kinetochore fiber movement occurs during both metaphase and anaphase-A in newt lung cell mitosis. J. Cell Biol. 119, 569–582.

O'Brien, E.T., Salmon, E.D., Walker, R.A., and Erickson, H.P. (1990). Effects of magnesium on the dynamic instability of individual microtubules. Biochemistry 29, 6648–6656.

Olmsted, J.B. (1981). Tubulin pools in differentiating neuroblastoma cells. J. Cell Biol. 89, 418–423.

Pfeffer, T.A., Asnes, C.F., and Wilson, L. (1976). Properties of tubulin in unfertilized sea urchin eggs: quantitation and characterization by the colchicine-binding reaction. J. Cell Biol. *69*, 599–607.

Pipeleers, D.G., Pipeleers-Marichal, M.A., and Kipnis, D.M. (1977a). Physiological regulation of total tubulin and polymerized tubulin in tissues. J. Cell Biol. *74*, 351–357.

Pipeleers, D.G., Pipeleers-Marichal, M.A., Sherline, P., and Kipnis, D.M. (1977b). A sensitive method for measuring polymerized and depolymerized forms of tubulin in tissues. J. Cell Biol. *74*, 341–350.

Rieder, C.L. (1977). An in vitro light and electron microscopic study of anaphase chromosome movements in normal and temperature elevated *Taricha* lung cells. Doctoral Dissertation, University of Oregon, Portland.

Rieder, C.L., Davison, E.A., Jensen, L.C., Cassimeris, L., and Salmon, E.D. (1986). Oscillatory movements of monooriented chromosomes and their position relative to the spindle pole result from the ejection properties of the aster and half-spindle. J. Cell Biol. *103*, 581–591.

Rothwell, S.W., Gasser, W.A., and Murphy, D.B. (1986). End-to-end annealing of microtubules in vitro. J. Cell Biol. *102*, 619–627.

Salmon, E.D. (1989). Microtubule dynamics and chromosome movement. In: Mitosis: Molecules and Mechanisms, ed. Hyam and Brinkley, Hyam and Brinkleys, New York: Academic Press Limited, 119–181.

Salmon, E.D., Leslie, R.J., Saxton, W.M., Karow, M.L., and McIntosh, J.R. (1984). Spindle microtubule dynamics in sea urchin embryos: Analysis using a fluorescein-labeled tubulin and measurements of fluorescence redistribution after laser photobleaching. J. Cell Biol. *99*, 2165–2174.

Sammak, P.J., and Borisy, G.G. (1988). Direct observation of microtubule dynamics in living cells. Nature *332*, 724–726.

Sammak, P.J., Gorbsky, G.J., and Borisy, G.G. (1987). Microtubule dynamics in vivo: a test of the mechanisms of turnover. J. Cell Biol. *104*, 395–405.

Sawin, K.E., and Mitchison, T.J. (1991). Polewards microtubule flux in mitotic spindles assembled in vitro. J. Cell Biol. 941–954.

Saxton, W.M., Stemple, D.L., Leslie, R.J., Salmon, E.D., Zavortink, M., and McIntosh, J.R. (1984). Tubulin dynamics in cultured mammalian cells. J. Cell Biol. *99*, 2175–2186.

Schulze, E., and Kirschner, M. (1988). New features of microtubule behaviour observed in vivo. Nature *334*, 356–359.

Shelden, E., and Wadsworth, P. (1993). Observation and quantification of individual microtubule behavior in vivo: microtubule dynamics are cell type specific. J. Cell Biol. *120*, 935–945.

Simon, J.R., Parsons, S.F., and Salmon, E.D. (1992). Buffer conditions and nontubulin factors critically affect the microtubule dynamic instability of sea urchin egg tubulin. Cell Motil. Cytoskeleton *21*, 1–14.

Skibbens, R.V., Skeen, V.P., and Salmon, E.D. (1993). Directional instability of kinetochore motility during chromosome congression and segregation in mitotic newt lung cells: A push-pull mechanism. J. Cell Biol. *122*, 859–876.

Snyder, J.A., and McIntosh, J.R. (1975). Initiation and growth of microtubules from mitotic centers in lysed mammalian cells. J. Cell Biol. *67*, 744–760.

Spurck, T.P., Stonington, O.G., Snyder, J.A., Pickett, H.J.D., Bajer, A., and Mole, B.J. (1990). UV microbeam irradiations of the mitotic spindle. II. Spindle fiber dynamics and force production. J. Cell Biol. *111*, 1505–1518.

Stemple, D.L., Sweet, S.C., Welsh, M.J., and McIntosh, J.R. (1988). Dynamics of a fluorescent calmodulin analog in the mammalian mitotic spindle at metaphase. Cell Motil. *9*, 231–242.

Vale, R.D. (1991). Severing of stable microtubules by a mitotically-activated protein in *Xenopus* extracts. Cell *64*, 827–839.

Vandre, D.D., and Borisy, G.G. (1985). The interphase-mitosis transformation of the microtubule network in mammalian cells. In: Cell Motility: Mechanism and Regulation, ed. H. Ishikawa, S. Hatano, and H. Sato, H. Ishikawa, S. Hatano, and H. Satos, Tokyo: University of Tokyo Press, 389–401.

Verde, F., Dogterom, M., Stelzer, E., Karsenti, E., and Leibler, S. (1992). Control of microtubule dynamics and length by cyclin A- and cyclin B-dependent kinases in *Xenopus* egg extracts. J. Cell Biol. *118*, 1097–1108.

Verde, F., Labbé, J., Dorée, M., and Karsenti, E. (1990). Regulation of microtubule dynamics by cdc2 protein kinase in cell-free extracts of *Xenopus* eggs. Nature *343*, 233–343.

Voter, W.A., O'Brien, E.T., and Erickson, H.P. (1991). Dilution-induced disassembly of microtubule: relation to dynamic instability and the GTP cap. Cell Motil. *18*, 55–62.

Wadsworth, P., and Salmon, E.D. (1986a). Analysis of the treadmilling model during metaphase of mitosis using fluorescence redistribution after photobleaching. J. Cell Biol. *102*, 1032–1038.

Wadsworth, P., and Salmon, E.D. (1986b). Microtubule dynamics in mitotic spindles of living cells. Ann. NY Acad. Sci. *466*, 580–592.

Walker, R.A., O'Brien, E.T., Pryer, N.K., Soboeiro, M.F., Voter, W.A., Erickson, H.P., and Salmon, E.D. (1988). Dynamic instability of individual microtubules analyzed by video light microscopy: rate constants and transition frequencies. J. Cell Biol. *107*, 1437–1448.

Walker, R.A., Pryer, N.K., and Salmon, E.D. (1991). Dilution of individual microtubules observed in real time in vitro: evidence that cap size is small and independent of elongation rate. J. Cell Biol. *114*, 73–81.